

# Erosion Mechanism of Claypan Soils in Southeastern Kansas

Mark A. Mathis II<sup>1</sup>, Tri V. Tran<sup>2</sup>, Stacey E. Tucker-Kulesza<sup>3</sup>, and Gretchen F. Sassenrath<sup>4</sup>

<sup>1</sup> Master's Student, S.M.ASCE, Department of Civil Engineering, Kansas State University, Manhattan, KS-66502. Email: mathisii@ksu.edu

<sup>2</sup> Ph.D. Candidate, Department of Civil Engineering, Kansas State University, Manhattan, KS-66502. Email: tritrans@k-state.edu

<sup>3</sup> Ph.D., P.E., M.ASCE, Assistant Professor, Department of Civil Engineering, Kansas State University, Manhattan, KS-66502. Email: sekulesza@ksu.edu

<sup>4</sup> Ph.D., Associate Professor, Department of Agronomy, Kansas State University, Manhattan, KS. Email: gsassenrath@ksu.edu

## ABSTRACT

Claypan soils cover approximately 40,469 km<sup>2</sup> in the United States and are characterized by a highly impermeable layer within 0.5 m from the ground surface. This impermeable layer acts as a barrier for infiltrating water, which may increase erosion rates and sediment transport. Two of the main problems associated with these processes are abutment scour and reservoir sedimentation. This study focuses on the undermining of surficial soils due to an impermeable claypan layer in Southeastern Kansas. The potential areas of critical soil loss and hydrologic flow patterns were determined using LiDAR-derived digital elevation maps across two 0.45 km<sup>2</sup> sites. These sites were located in areas of both high and low elevation. Electrical resistivity tomography (ERT) was used in areas identified with LiDAR to measure the depth to claypan, which was originally believed to be uniform across the region. The results indicated that the claypan layer was located from 0.5 to 0.75 m and dissipated moving across the site from an area of high elevation to an area of low elevation. Undisturbed soil samples were collected based on the ERT analysis, in areas with and without the claypan. An erosion function apparatus (EFA) was used to directly measure erosion due to sheet flow and to identify the controlling mechanism causing surficial soil loss. The knowledge gained on claypan erosion mechanisms will improve the prediction of near surface soil erodibility to support aging infrastructure.

## INTRODUCTION

Soil loss is an environmental problem which impacts all aspects of society from impaired water resources to infrastructure stability. Claypan soils are characterized by a highly impermeable layer below surficial soil and cover approximately 40,469 km<sup>2</sup> of the United States (Jamison et al., 1968; Blanco-Canqui et al., 2002). Erosion in claypan soils reduces water quality by fostering toxic algal blooms and limiting reservoir capacity by sedimentation (Kansas Water Office, 2016). The erosion in claypan soils ultimately decreases the surficial soil depth exposing the impermeable claypan layer at the surface. The objective of this research was to delineate the variability of soil properties, including soil erodibility, in claypan soils. Understanding how soil properties change within the soil profile is critical to understanding the processes exacerbating soil loss in claypan regions. To do this, field geophysical methods (apparent electrical conductivity (ECA) measurements and

electrical resistivity tomography (ERT) surveys) were used to determine the location of samples, erosion tests were used to determine soil properties.

Soil conductivity is a measurement of how well a representative volume of soil conducts electricity. Soil conductivity is a function of the soil clay content, moisture content, bulk density, temperature, and salinity (Rhoades et al. 1989). As such it has become a valuable tool for mapping soil variability near the surface. The main advantage of a soil conductivity measurement is it is capable of collecting data over large areas as opposed to discrete sampling methods. The disadvantage of a soil conductivity measurement is that data are only collected near the surface (0.30 – 0.80 m), the measurements are relative measurements, and it has limitations for studying intrinsic soil properties.

Electrical resistivity tomography (ERT) is a popular near-surface geophysical method commonly used to delineate soil stratigraphy (Groves et. al., 2011). The term “near-surface” generally means down to approximately 9 m in the subsurface. ERT has been used for identifying bridge foundations (Arjwech et al., 2013), mapping landfills (Bernstone et al., 2000), predicting soil erodibility (Karim & Tucker-Kulesza, 2018), and geotechnical site characterization (Hiltunen and Roth, 2003). Electrical resistivity is the reciprocal measurement of electrical conductivity; therefore both systems measure differences in the same soil properties. ERT measurements are different than surface electrical conductivity measurements because ERT collects a “slice” of data into the subsurface, as opposed to only changes at the surface. Relative measurements, similar to those collected in an electrical conductivity survey, are collected; however, in ERT studies the data are mathematically inverted to yield the true electrical resistivity of the soil with depth. This allows an interpretation of the changing soil properties with depth to reduce the required amount of sampling. A disadvantage of an ERT survey is that the data acquisition is stationary so mapping a large site in one day is typically not feasible. Therefore, electrical conductivity measurements were used to guide the location of ERT surveys in this project.

The erosion function apparatus (EFA) test directly measures the erosion rate of undisturbed soil samples due to sheet flow to obtain the critical shear stress. The critical shear stress is the applied hydraulic stress at which a soil starts to erode (Bernhardt et al., 2011) and a higher critical shear stress indicates that a soil is more resistant to erosion. EFA tests were used to identify the variability in soil erosion with depth in claypan soils. This study combined surface electrical conductivity measurements, ERT surveys, and EFA tests to characterize where soil erosion was likely occurring. There was a need to identify how, where, and why claypan soils are eroding to understand the erosion mechanisms before only the impermeable layer remains.

The research methodology, including field work, study site, and EFA test, is followed by this introduction. Next, the results and discussion from the two sites are shown. This paper ends with conclusions, including future work.

## METHODOLOGY

**Geophysical methods.** Soil apparent electrical conductivity ( $EC_a$ ) was mapped using a direct contact sensor (Veris Industries, Salina, Kan.) in concert with a GPS system mounted on a tractor. The system uses six 0.43 m diameter disc electrodes that remain in direct contact with the soil surface. Two discs serve as the current source/sink and four measure the resulting voltage potential. The disc spacing controls the depth of penetration of the electrical survey, which were 0.30 m and 0.80 m vertical depth in the soil profile in this study. The minimum depth, 0 m to 0.30

m, was used because this is the depth of interest for this study.  $EC_a$  measurements were mapped in SMS Advanced (AgLeader, Ames, Iowa). The boundary condition for a designated “high  $EC_a$ ” area and “low  $EC_a$ ” area was determined using the electrical conductivity data at both sites.

ERT surveys were used to measure the apparent resistivity of the underlying soil profile. ERT surveys utilize two electrodes as the current/sink and at least two electrodes to measure the resulting voltage potential. Each apparent resistivity measurement is considered the resistivity that would have been measured if the earth were homogenous (Everett, 2013), measured in Ohm-m. ERT surveys collect apparent resistivity measurements using multiple electrodes in arbitrary geometric patterns (Dailey et al., 2005). The spatial distribution of electrodes used determine the depth of the resistivity measurement into the soil profile. The resulting dataset is a map of the apparent resistivity measurements in the subsurface.

All ERT data must undergo an inversion process to determine the true resistivity distribution in the subsurface. A measure of the goodness of fit between the calculated apparent resistivity data for the inversion and measured apparent resistivity data is determined by the L2-norm and RMS error. Typically RMS less than 3% is considered an excellent fit, 3-5% a good fit, and 6-10% is acceptable but should be interpreted with caution (Tucker et al., 2015). The objective in the ERT inversion was to find the solution that fits within the following criterion; less than 5% RMS and L2-norm less than one. The RMS error and L2-norm for the ERT surveys presented in this paper indicate excellent or good agreement between measured and calculated resistivity according to Tucker et al. (2015).

**Experimental setup.** Two, 0.45 km<sup>2</sup> sites located near Bartlett, KS were selected for this research. The ERT surveys began in a high  $EC_a$  area and ended in a low  $EC_a$  area. This was done to show the change in soil subsurface material. Setup for an ERT survey included attaching 56 stainless steel electrodes to 56 stainless steel stakes and driving the stakes into the ground so that the electrodes sit just above the surface. The sequence of measurements, or array type, in an ERT survey affects the resolution of the results and the data collection time. A strong gradient was selected as it collects high resolution data near the surface in approximately one hour. The relative elevation of each electrode at the soil surface was measured using a Total Station survey. The commercial software EarthImager 2D (AGI, 2007) was used to invert the measured apparent resistivity data to the true resistivity of the subsurface. Soil samples were collected at both sites, guided by the ERT results, to determine soil erosion properties.

At site one, the electrode spacing was 0.15 m which provided detailed information on the soil layers less than 1.5 m. A total of eight ERT surveys was conducted but only the ERT surveys that identified the transition area between a high and low  $EC_a$  are shown in this paper. The ERT surveys overlap with each other such that the midpoint of the first ERT survey was the starting point for the second ERT survey and the midpoint of the second ERT survey was the starting point for the third ERT survey. The midpoint of each ERT survey is highlighted by a red dashed line.

The electrode spacing was 0.30 m at site two, which provided detailed information on the soil layers less than 4.0 m. The electrode spacing was increased to utilize a more efficient procedure to identify the transition area while reducing the number of ERT surveys. A total of three ERT surveys were conducted to identify the transition area between high  $EC_a$  and low  $EC_a$  at site two. The ERT surveys were setup in such a way that the end of the first ERT survey was the starting point for the second ERT survey and the end of the second ERT survey was the starting point for the third ERT survey.

**Erosion Function Apparatus (EFA) Test.** The EFA was developed to directly measure the erosion rate of soil samples, initially for bridge scour. The procedures described by Briaud et al. (2001) and Tran et al. (2017) were utilized in this study. In an EFA test, a thinned walled Shelby tube with the field-retrieved sample was placed into an opening in the flume with the cross sectional of 101.6 x 50.8 mm. A pump was used to drive the flow over the top of the soil sample in the flume. As the soil eroded, a piston was pushed upward to extrude the sample from the Shelby tube such that the top of the sample was always kept flush with the flume bottom during testing. The temperature of the water in the flume was maintained at the constant number. Each sample was tested for 50 minutes at water velocities of 1, 2, 3, and 4 m/s. After each water velocity tests, two photos of the soil surface were taken and processed with a custom photogrammetry computational program to compute the soil surface roughness (as described by Tran et al. (2017)). This roughness was used to get the friction factor,  $f$ , in the Moody chart (Moody 1944) and the shear stress in the EFA testing was obtained as

$$\tau_e = \frac{1}{8} f \rho v^2 \quad (1)$$

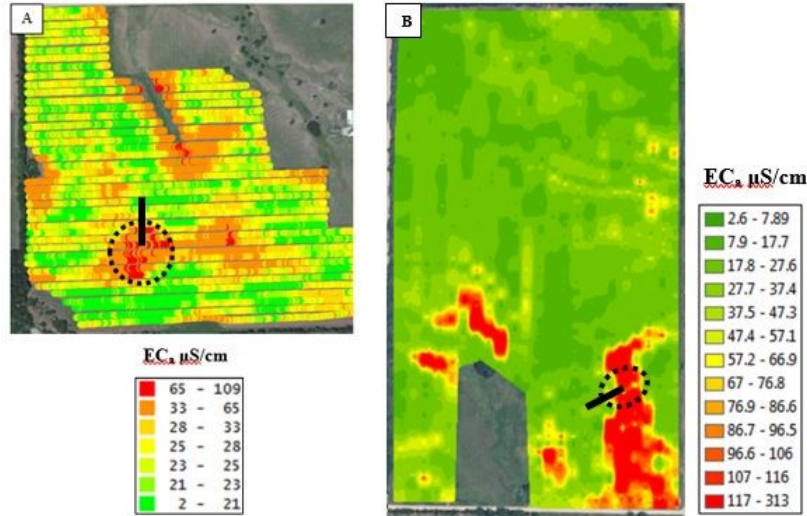
where  $\rho$ , is the mass density of the water and  $v$  is the flow velocity. The erosion rate at each velocity is calculated as

$$\dot{z} = \frac{h}{t} \quad (2)$$

where  $h$  is the length of soil sample eroded and  $t$  is the testing time. These data were used to create a plot of erosion rate and shear stress for each sample.

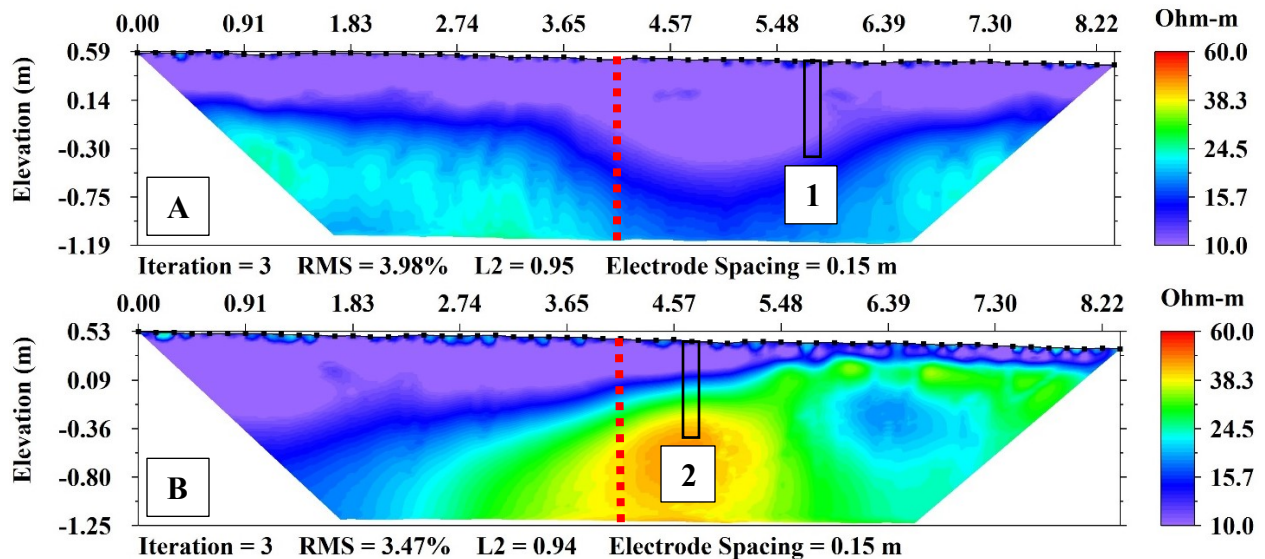
## RESULTS

Fig. 1A and 1B shows the  $EC_a$  measurements of the upper soil layer measured at approximately 0.30 m depth in the soil profile sites one and two, respectively. Fig. 1A shows high  $EC_a$  from 65  $\mu\text{S}/\text{cm}$  to 109  $\mu\text{S}/\text{cm}$  in the center of site one, highlighted by the dashed black circle. Fig. 1B shows high  $EC_a$  from 117  $\mu\text{S}/\text{cm}$  to 313  $\mu\text{S}/\text{cm}$  in the southeast section of site two, shown by the dashed black circle. Higher  $EC_a$  measurements were correlated to higher clay content in clay-pan soils (Kitchen et al., 2005). The variability in near surface soil characteristics within the field was evident from the  $EC_a$  at both sites. ERT surveys were conducted to examine changes in the soil profile to better define the factors contributing to the variability. The solid black line in Fig. 1A and Fig. 1B shows where the ERT surveys were conducted at each site moving from a high to low  $EC_a$  area.



**Fig. 1: (A) Site one apparent electrical conductivity (EC<sub>a</sub>) map. (B) Site two apparent electrical conductivity (EC<sub>a</sub>) map. Solid black lines show ERT survey locations.**

The ERT measurements of the high EC<sub>a</sub> area at site one are shown in Fig. 2A. The upper layer, shown in purple, had a measured resistivity of 10 Ω-m or less from the surface to approximately 0.14 m below the surface. The second layer had a measured resistivity between 12.9 Ω-m and 24.5 Ω-m and was 0.14 m from the surface to the bottom of the survey. The ERT measurements of the transition area (i.e. between a high and low EC<sub>a</sub> area) are shown in Fig. 2B. In this survey the low resistivity layer (10 Ω-m or less) thins from 0.89 m to less than 0.31 m in thickness as the region of measurements moves towards a low EC<sub>a</sub> area. The measured resistivity was between 38.3 Ω-m and 49.2 Ω-m between the 3.65 marker and the 5.48 marker and starting -0.36 m below the surface. The ERT measurements of the low EC<sub>a</sub> area are shown in Fig. 2C. The low resistivity layer (10 Ω-m or less), was still present near the surface, however it was relatively thinner and appeared to dissipate across the profile compared to Fig. 2A and 2B.



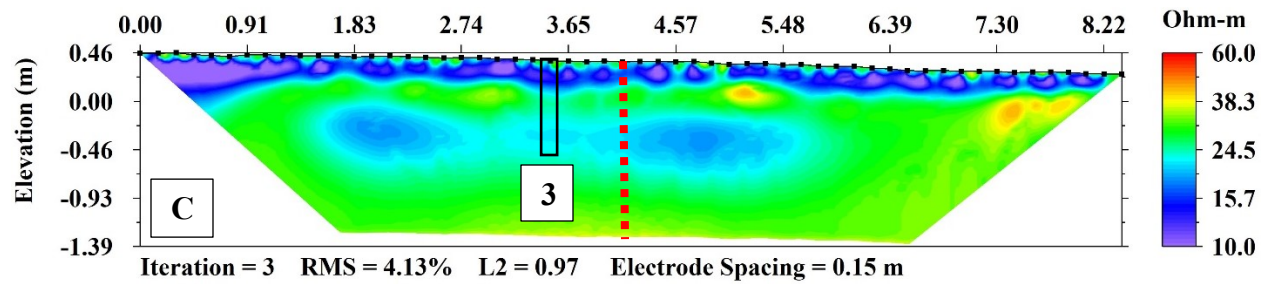


**Fig. 2: Site one ERT survey results: (A) High EC<sub>a</sub> area; (B) Transition area between a high and low EC<sub>a</sub> area; (C) Low EC<sub>a</sub> area.**

The rectangles drawn in Fig. 2 show the soil sampling locations. One sample was collected from the high, transition, and low EC<sub>a</sub> areas using a plastic tube via a direct push method. All samples were classified according to Unified Soil Classification System (USCS). Each sample was 91 cm long and 7.6 cm in diameter. Undisturbed soil samples were collected adjacent to the high, transition, and low EC<sub>a</sub> areas using 30 cm long, 7.6 cm thinned walled Shelby tubes via a direct push method. The undisturbed samples were taken within close proximity (0.61 m - 1.2 m) to the samples collected in plastic tubes and were assumed to have the same soil classification corresponding to the nearest classified soil sample. The index properties of the samples are shown in Table 1. All samples in Fig. 2 had two layers. A top layer (noted as T) and bottom layer (noted as B). All top layers were classified as lean clay (CL) and all bottom layers classified as fat clay (CH). Table 1 also includes the electrical resistivity of each sample and erosion data.

**Table 1. Soil parameters and classification of site one.**

Sample	Sample Depth (m)	ER (Ωm)	ω (%)	LL	PI	P <sub>200</sub>	USCS Classification	Erodibility	Critical Shear Stress (N/m <sup>2</sup> )
1-T	0.24	11.3	27.26	30	14	89	CL	Low	17.98
1-B	0.67	12.6		53	29	85	CH		
2-T	0.12	14.5	21.17	38	21	89	CL	Moderate	4.49
2-B	0.79	31.3		73	52	83	CH		
3-T	0.24	20.5	25.84	27	9	89	CL	Moderate	5.12
3-B	0.67	21.8		76	51	95	CH	Low	73.91

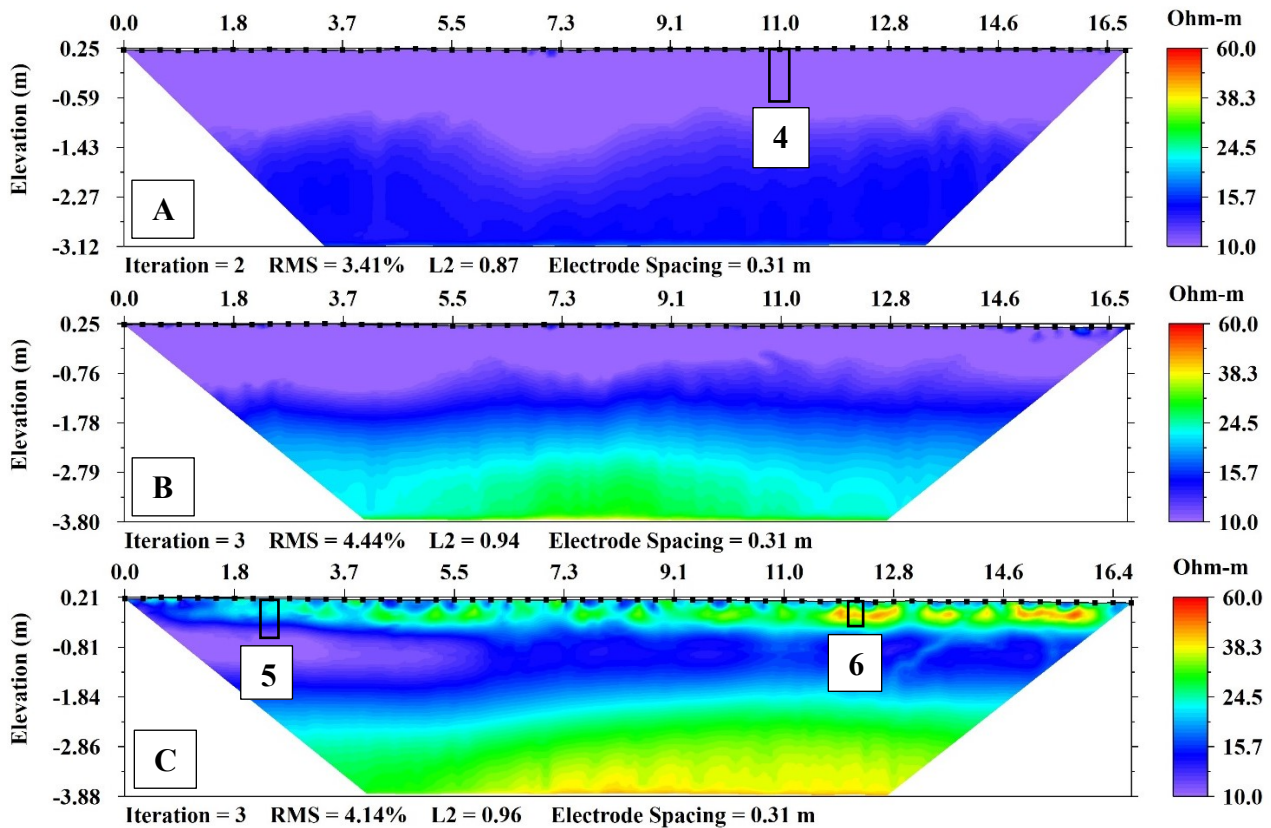
\*Note: T=top of sample; B=bottom of sample

Fig. 3A is the ERT measurement at a high EC<sub>a</sub> area at site two. Two layers are present in Fig. 3A. The upper layer, shown in purple, had a measured resistivity layer of 10 Ω-m or less at the surface to approximately 1.43 m below the surface. The low resistivity layer overlies a layer, shown in dark blue, with a measured resistivity between 12.9 Ω-m and 15.7 Ω-m and is -1.43 m below the surface to the bottom of the measured survey. The ERT measurements in Fig. 3B had an upper layer, shown in purple, with a resistivity layer of 10 Ω-m or less to approximately -1.27 m below the surface. The low resistivity layer (10 Ω-m or less) overlies a high resistivity layer between 12.9 Ω-m and 38.3 Ω-m from -1.27 m below the surface to the bottom of the measured survey. The ERT measurements of a low EC<sub>a</sub> area, shown in Fig. 3C, shows a layer with a resistivity between 15.7 and 49.2 Ω-m at the surface overlying a layer with a thickness of 2.14 m and a measured resistivity of 15.7 Ω-m or less. A layer with a measured resistivity between 20.1

$\Omega$ -m and 38.3  $\Omega$ -m is -1.84 m below the surface to the bottom of the measured survey. The rectangles drawn in Fig. 3 shows the location of samples collected at the site. The same sampling procedure was followed from site one. The index properties for the samples are shown in Table 2. Sample four (4), shown in Fig. 3A, had one layer that was a clean clay (CL). Sample five (5), shown in Fig. 3C, had 2 layers (CL over CH) and sample six (6) had one CL layer.

**Table 2. Soil parameters and classification of site two.**

Sample	Sample Depth (m)	ER ( $\Omega$ m)	$\omega$ (%)	LL	PI	P <sub>200</sub>	USCS Classification	Erodibility	Critical Shear Stress (N/m <sup>2</sup> )
4	0.91	5.8	24.66	31	14	88	CL	Low-Moderate	4.87
5-T	0.40	22.4	31.51	28	10	86	CL	Moderate	1.03
5-B	0.21	13.1		54	33	92	CH		
6	0.46	31.6	35.58	30	11	85	CL	Moderate	4.74



**Fig. 3: Site two ERT survey results: (A) High EC<sub>a</sub> area; (B) Transition between High/Low EC<sub>a</sub>; (C) Low EC<sub>a</sub> area.**

Surface soil erosion tests were performed under six different velocities from 1 to 6 m/s to measure the critical shear stress of the soils at the two sites. The samples were allowed to erode for 50 minutes under each velocity. Note that when sample 2 was tested under 5 m/s, clumps of soil were plucked from the Shelby tube, so the shear stress could not be calculated and there was

not enough remaining sample for testing at 6 m/s flow velocities. As mentioned earlier, sample 3 had two layers so the top (T) and bottom (B) were tested individually. All erosion points were plotted according to HEC-18 erodibility categorization, which does not show points corresponding to zero erosion rate as it is a log-log plot.

There was no measurable erosion of the sample 1 until 6 m/s and sample 3(B) did not erode until 5 m/s. Fig. 4A shows that sample 1 was the least erodible compared to the rest of the samples at site one and it was classified as very low to low erodibility according to HEC-18 erodibility categorization. Note that the critical shear stress in Table 1 was the shear stress that corresponded 0.1 mm/h erosion rate (Briaud et al. 2001). The critical shear stress for sample 3(B) was higher than sample 1 even though they were classified as the same category. This indicates that the sample 3(B) was more erosion resistant. Fig. 4B shows the EFA results for all samples from site two. Sample 5 and 6 had zero erosion at 1 m/s, whereas no measurable erosion (via extrusion in the EFA) occurred until 3/s flow velocity for sample 4. Sample 5 was comparatively more erodible than the other samples as the critical shear stress had the lowest value in Table 2. Sample 5 had a lower erosion rate than sample 6 at 2 and 3 m/s flow velocity; however, at higher water velocities (5 and 6 m/s), the erosion rates of sample 5 were significantly higher (more than 8 times) than the erosion rate of sample 6. All samples at site 2 were more erodible than site 1.

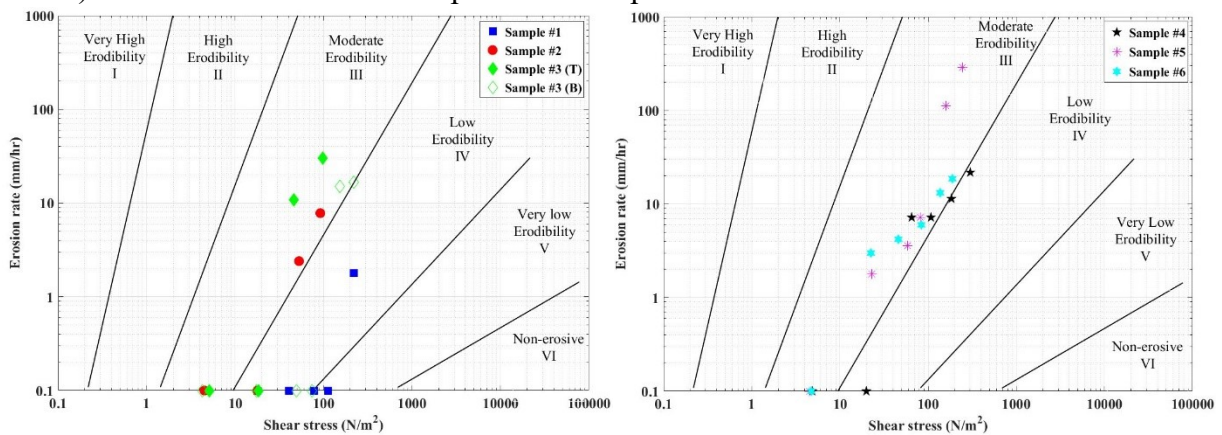


**Fig. 4: Site one EFA results; (B) Site two EFA results**

## DISCUSSION

Fig. 2A and 3A show the electrical resistivity with depth in areas of highest conductivity according to the  $EC_a$  measurements in Fig. 1. Soil samples collected from these regions (i.e. Sample 1 and Sample 4) were the most resistant to erosion. The measured critical shear stress of Sample 1-T was  $17.98 \text{ N/m}^2$  and Sample 4 was  $4.87 \text{ N/m}^2$ , therefore Sample 1-T was more erosion resistant than Sample 4. These are areas where the claypan has been exposed due to years of surface erosion. This is likely causing water to flow laterally along the clay surface, increasing water flow to the other regions of the site, including towards the low  $EC_a$  region. Researchers have established that surficial soil is diminishing in the claypan region (Gantzer et al., 1991; Kitchen et al., 1999; Jung et al., 2005; Jiang et al., 2007); increasing flow from one region of the site to another where soils erode more easily is likely exacerbating this process.

Samples 2 and 3 were collected from regions where there was less clay near the surface (visually the purple sections in Fig. 2 B and C), and the samples were more erodible than Sample 1. Interestingly, Sample 3 was split into top and bottom for EFA testing and the bottom of the sample had the highest critical shear stress of all samples (73.91 N/m<sup>2</sup>). The next phase of this research explores if additional surficial soil may be diminishing due to a deeper impermeable layer, causing soil loss by undermining erosion. Finally, Samples 5 and 6 were collected from areas at site two where there was not a low resistive layer at the surface (indicative of claypan described above). The ERT profile shows what appears to be a claypan layer that is 2.14 m thick starting approximately 0.8 m in the subsurface. The EFA results indicated that the soil on top of this clay layer was the most erosive. Sample 5 had the lowest critical shear stress of 1.03 Pa and Sample 6 4.74 Pa. An additional EFA test is needed on the lower resistivity layer in Fig. 3C, however these results support the working hypothesis that soil loss may be exacerbated by a deeper impermeable clay layer and that without intervention this impermeable layer will be at the surface as in Fig. 2A, 3A, and 3B.

## CONCLUSIONS

The data from this study show that the clay layer is spatially variable. The extent to which the spatial variability of the clay layer may contribute to different rates of erosion of the overlying material. The range in shear stress between high and low EC<sub>a</sub> regions indicate that the rate and extent of soil erosion from within both sites will be highly variable based on subsoil composition. The impermeable clay layer is very resistant to erosion; however, it may enhance the rate of erosion of the surficial soil due to its impervious nature. Better understanding on the claypan erosion mechanisms will improve the prediction of near surface soil erodibility.

This paper presents the initial results in a study on erosion mechanisms in claypan soil. Future work includes two additional erosion tests. The jet erosion test (JET) will be used to simulate head cutting or free fall erosion and the hole erosion test (HET) will be used to measure the erosion susceptibility to undermining at the surficial soil/claypan interface. The HET will allow for a direct evaluation of soil piping. An additional geophysical measurement is planned to validate the predicted movement of water at the claypan interface.

## ACKNOWLEDGEMENTS

This research was funded by the National Science Foundation, Environmental Sustainability program. The authors gratefully acknowledge the support of the Kansas State University Women in Engineering Program. We gratefully acknowledge the cooperation of the participating farmer in providing us access to their land.

## REFERENCES

AGI (Advanced Geosciences, Inc.). (2008). *Instruction Manual for EarthImager 2D Version 2.4.0 Resistivity and IP Inversion Software*, Advanced Geosciences, Inc., Austin TX.

- Arjwech, R., Everett, M.E., Briaud, J.-L., Hurlebaus, S., Medina-Cetina, Z., Tucker, S., & Yousefpour, N. (2013). Electrical resistivity imaging of unknown bridge foundations, *Near Surf. Geophys.*, 11(6), 591-598. <http://doi.org/10.3997/1873-0604.2013023>
- Bernstone, C., Dahlin, T., Ohlsson, T., & Hogland, H. (2000). DC Resistivity mapping of internal landfill structures: Two pre-excavation surveys. *Environ. Geol.*, 39(3-4), 360-371. <https://doi.org/10.1007/s002540050015>
- Briaud, J. L., Ting, F., Chen, H. C., Cao, Y., Han, S. W., & Kwak, K. W. (2001). "Erosion Function Apparatus for Scour Rate Predictions." *Journal of Geotechnical and Geoenvironmental Engineering*, 127(2), 105–113. [https://doi.org/10.1061/\(ASCE\)1090-0241\(2001\)127:2\(105\)](https://doi.org/10.1061/(ASCE)1090-0241(2001)127:2(105))
- Daily, W., Ramirez, A., Binley, A., & LaBrecque, D. (2005). Electrical resistivity tomography: Theory and practice. In D.K. Butler(Ed.), *Near-surface geophysics* (13<sup>th</sup> ed., pp.525-550). Tulsa, OK: Soc. Exploration Geophysicists. <https://doi.org/10.1190/1.9781560801719.ch17>
- Everett, M.E. (2013). *Near-surface applied geophysics*. New York, NY: Cambridge University Press. <https://doi.org/10.1017/CBO9781139088435>
- Groves, P., Cascante, G., Dundas, D., & Chatterji, P. K. (2011). Use of geophysical methods for soil profile evaluation. *Canadian Geotech. J.*, 48(9), 1364-1377. <https://doi.org/10.1139/t11-044>
- Jiang, P., Anderson, S. H., Kitchen, N. R., Sadler, E. J., & Sudduth, K. A. (2007). Landscape and conservation management effects on hydraulic properties of a claypan-soil toposequence. *SSSAJ*, 71(3), 803-811. <https://doi.org/10.2136/sssaj2006.0236>
- Karim, M.Z. & Tucker-Kulesza, S. (2018). Predicting soil erodibility using electrical resistivity tomography. *J. Geotech. Geoenviron. Eng.* 144(4): 04018012. [https://doi.org/10.1061/\(ASCE\)GT.1943-5606.0001857](https://doi.org/10.1061/(ASCE)GT.1943-5606.0001857)
- Kitchen, N. R., Sudduth, K. A., Myers, D. B., Drummond, S. T., & Hong, S. Y. (2005). Delineating productivity zones on claypan soil fields using apparent soil electrical conductivity. *Comput. Electron. Agric.*, 46(1), 285-308. <http://dx.doi.org/10.1016/j.compag.2004.11.012>
- Rhoades, J. D., Manteghi, N. A., Shouse, P. J., & Alves, W. J. (1989). Soil electrical conductivity and soil salinity: New formulations and calibrations. *SSSAJ*, 53(2), 433-439. <https://doi.org/10.2136/sssaj1989.03615995005300020020x>
- Sassenrath, G. & Kulesza, S. (2017). Measuring soil electrical conductivity to delineate zones of variability in production fields. *Kansas Agricultural Experiment Station Reports*, 3(2), 1-17.

- Tran, T., Tucker-Kulesza, S., & Bernhardt, M. (2017). "Determining Surface Roughness in Erosion Testing Using Digital Photogrammetry." *Geotechnical Testing Journal*, 40(6), 917-927. <https://dx.doi.org/10.1520/GTJ20160277>
- Tucker, S. E., Briaud, J.-L., Hurlebaus, S., Everett Mark, E., & Arjwech, R. (2015). Electrical resistivity and induced polarization imaging for unknown bridge foundations. *J. Geotech. Geoenviron. Eng.*, 141(5). [https://doi.org/10.1061/\(ASCE\)GT.1943-5606.0001268](https://doi.org/10.1061/(ASCE)GT.1943-5606.0001268)
- Kansas Water Office. (2016). John Redmond dredging initiative. Retrieved from <http://www.kwo.org/projects/JohnRedmondDredging.html>
- Blanco-Canqui, H., Gantzer, C. J., Anderson, S. H., Alberts, E. E., & Ghidry, F. (2002). Saturated hydraulic conductivity and its impact on simulated runoff for claypan soils. *SSSJ*, 66(5), 1596-1602. <https://doi.org/10.2136/sssaj2002.1596>